East European Journal of Physics. 1. 256-260 (2026)
DOI:10.26565/2312-4334-2026-1-28 ISSN 2312-4334

ENHANCING THE YIELD OF CARBON NANOTUBES THROUGH THE NANOCATALYST-SUBSTRATE INTERFACE

Ilyos J. Abdisaidov*, Sevara G. Gulomjanova, Ilyos Kh. Khudaykulov, Khatam B. Ashurov
Institute of Ion-Plasma and Laser Technologies named after U.A. Arifov, Academy of Sciences of the Republic of Uzbekistan, 100125, Durmon yuli st. 33, Tashkent, Uzbekistan
**Corresponding Author-mail: ilyos.abdisaidov@gmail.com*
Received August 24, 2025; revised December 19, 2025; accepted January 19, 2026

In this study, the effect of the nanocatalyst/substrate interface on the yield and quality of carbon nanotubes (CNTs) synthesized by chemical vapor deposition (CVD) was investigated. Nickel oxide (NiO) nanoparticles were prepared using the sol–gel spin-coating method and deposited as thin films with different masses (66 mg, 99 mg, and 132 mg) on SiO_2/Si substrates with an identical surface area of 12,56 cm^2. The NiO nanoparticle thin films on the substrate surface were then placed into a CVD reactor and reduced in a hydrogen atmosphere, resulting in the formation of nickel nanoparticles that acted as active catalysts during CNTs synthesis. Ethanol vapor was used as the sole carbon source without any carrier gas, which enabled precise and comparative evaluation of the CNTs yield. X-ray diffraction (XRD) and Raman spectroscopy were employed to characterize the obtained CNTs. XRD results showed that CNTs with high crystallinity were produced when a 51,7 mg catalyst thin film was used. Raman spectroscopy confirmed the presence of RBM, G, D, and G′ peaks characteristic of CNTs structures. Increasing the catalyst mass led to a rise in RBM frequency and a decrease in CNTs diameter. However, an increase in catalyst mass also caused a reduction in CNTs yield. The highest yield (445%) was observed for Ni nanocatalysts with a mass of 51,7 mg. These findings demonstrate that the thickness of the catalyst layer and its surface distribution density on the substrate play a crucial role in determining the growth efficiency and structural quality of CNTs.
Keywords: *Carbon nanotubes; NiO catalyst; Sol-gel method; CVD; Substrate–nanocatalyst interface; RBM; Yield*
PACS: 61.46-w, 61.46.+w, 61.46.Np

INTRODUCTION

CNTs are nanoscale materials characterized by high strength, light weight, and unique electronic, thermal, and optical properties. They possess significant potential for application in future technologies, particularly in nanoelectronics, sensing, energy storage devices, hydrogen energy, biomedicine, and nanocomposites [1–3]. The synthesis of CNTs has attracted considerable attention from researchers, especially vertically aligned nanotubes, which offer major technological advantages. However, achieving high-quality growth and high productivity requires the synergistic interaction of multiple factors, notably the nature of the catalyst, the substrate material, synthesis conditions, and the properties of the interface [4, 5].

The growth of CNTs is typically carried out using the CVD method, in which nanoparticles of the nanocatalyst play an active role on the substrate surface. The nanocatalyst-substrate interface (i.e., the interaction between them, contact angle, surface energy, and structural stability) determines the growth mechanism and type of CNTs (single-walled or multi-walled) [6,7].

Several studies have shown that the smaller the contact angle at the interface, the better the spreading of catalyst particles on the substrate, which ensures their superior thermal stability [8]. This is a critical condition for the aligned and continuous growth of nanotubes. For example, in CNTs synthesized on SiO_2/Si substrates using Ni or Fe catalysts, interfacial forces and excess charge distribution in the substrate directly influenced growth efficiency [9–11].

Additionally, the presence of an intermediate oxide layer (e.g., Al_2O_3, MgO, and TiO_2) on the substrate can prevent catalyst agglomeration and maintain its activity over an extended period [12]. In such cases, the interface between the substrate surface and the catalyst acts as an active site. Certain studies have also revealed that the presence of Na^+ or Mg^{2+} ions in the substrate composition can affect the catalytic process, as these ions participate in diffusion processes and alter the electronic structure of the interface [13].

The size, distribution, and isolated positioning of catalyst particles on the substrate surface are also of critical importance. Their activity depends not only on chemical composition but also on the binding forces with the substrate and the interface energy [14]. Therefore, engineering the nanocatalyst-substrate interface becomes essential for controlling the synthesis process. Recent research has demonstrated that improving the interface can significantly enhance the yield of carbon nanotubes [15].

This study focuses specifically on analyzing the properties of the nanocatalyst–substrate interface to improve the growth and efficiency of carbon nanotubes.

EXPERIMENTAL PROCEDURE

a) Catalyst preparation.

The synthesis of NiO nanoparticles was carried out using the sol-gel spin coating method, a schematic of the synthesis process is shown in Figure 1.

Cite as: I.J. Abdisaidov, S.G. Gulomjanova, I.Kh. Khudaykulov, Kh.B. Ashurov, East Eur. J. Phys. 1, 256 (2026), https://doi.org/10.26565/2312-4334-2026-1-28

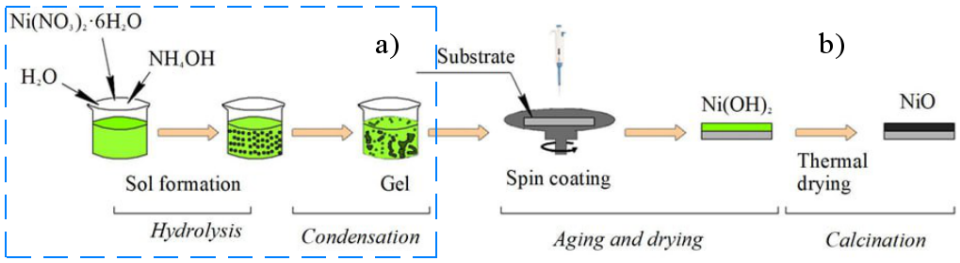

Figure 1. Schematic illustration of the formation of thin NiO layers with varying masses on the substrate surface

As seen in Figure 1, the formation of the NiO layer on the substrate surface consists of two steps:

a) preparation of a metal hydroxide sol using the sol–gel method [16];

b) formation of a thin metal hydroxide film on the substrate surface during the spin-coating process.

Initially, nickel nitrate [$Ni(NO_3)_2 \cdot 6H_2O$], ammonium hydroxide (NH_4OH), and deionized water were used as the starting reagents. An aqueous solution containing $Ni(NO_3)_2 \cdot 6H_2O$ and ammonium hydroxide in a 1:2 molar ratio was prepared and placed in a glass flask. The mixture was continuously stirred for 2 hours at a temperature of 85°C using a magnetic stirrer. After stirring, the resulting suspension was cooled to room temperature and allowed to age for 20 hours. The resultant $Ni(OH)_2$ was then used for the synthesis of carbon nanotubes. $Ni(OH)_2$ was applied onto three SiO_2/Si substrates with identical surface areas (12,56 cm^2) in different masses, and subsequently calcined in a SNOL laboratory furnace at 400°C for 2 hours. This thermal treatment resulted in the formation of a thin NiO layer on the surface of the substrates.

b) Synthesis of carbon nanotubes.

CNTs were synthesized using the CVD method. Ethanol vapor was employed as the hydrocarbon source, and no carrier gas was used to ensure accurate assessment of the ethanol vaporization efficiency and conversion. Nickel (Ni) nanoparticles, which were obtained by hydrogen reduction of the NiO synthesized through the sol-gel spin coating method, served as the catalyst for the CNTs growth. This process was carried out in the temperature range of 200÷400°C at a heating rate of 5°C/min. As a result, thin Ni nanocatalyst layers with different masses (51,7 mg, 77,6 mg, and 103 mg) were formed on the substrate surfaces. The synthesis process was then conducted at 500°C for 0,5 hours.

RESULTS AND DISCUSSION

In this study, the characterization of single-walled carbon nanotube (SWCNTs) samples was performed using XRD in order to acquire indirect information regarding the properties of the catalyst used. The XRD patterns, as shown in Figure 2, were obtained utilizing a Rigaku Smartlab X-ray diffractometer, employing CuKα radiation with a wavelength of 0.15405 nm, along with a Kβ filter to ensure accurate measurements. The experimental setup included a tube current of 50 mA and a tube voltage of 40 kV, optimizing the diffraction process. A range of angular 2θ values between 5° and 100° was explored, with the scanning rate set at 3° per minute. To ensure high precision in the analysis, the resolution of the 2θ scan was consistently maintained at 0.01°, providing a detailed and reliable dataset for subsequent analysis.

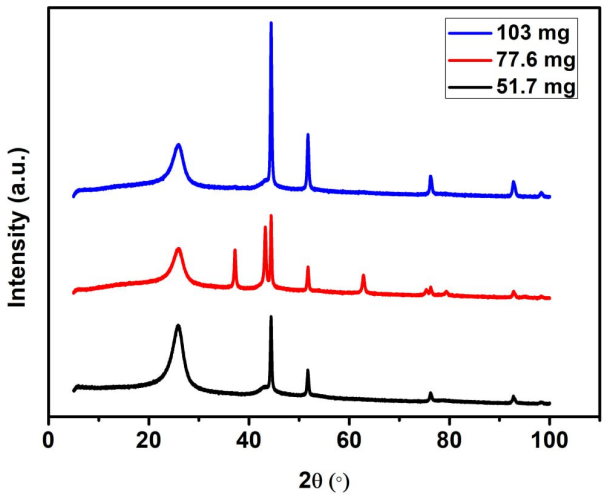

Figure 2. XRD diffractograms of the synthesized CNTs

Figure 2 presents the XRD spectra of CNTs synthesized via the CVD method on SiO_2/Si substrates of identical size, using a Ni nanocatalyst with varying thicknesses. It is important to note that the use of SiO_2/Si substrates - specifically the presence of a natural SiO_2 layer (~360 nm) on the Si surface prevents stress formation on the Si substrate at elevated temperatures and inhibits the formation of nickel silicide [17, 18]. The XRD analysis revealed several peaks

corresponding to the carbon structure, specifically the (002), (101), (201), (020), (222), and (112) planes. Of these, the (002) peak is considered the most significant, while the other peaks are less relevant [19]. This prominent (002) peak is located at approximately 2θ ≈ 25,89°, and its intensity can be used as an indicator of the crystallinity of the CNTs. In addition to the CNTs related peaks, the XRD spectrum also revealed the presence of Ni and NiO phases associated with the catalyst material. At temperatures above 400°C, nickel reacts with oxygen to form NiO, resulting in low-intensity NiO traces appearing in the diffraction spectrum [20]. According to the XRD analysis, a catalyst mass of 51,7 mg corresponding to a specific catalyst layer thickness leads to the formation of CNTs with higher crystallinity.

The samples were analyzed using Raman spectroscopy, produced by Renishaw, UK. Excitation was provided by a RL532 Class 3B laser, with a radiation wavelength of 532 nm. For the measurements, a diffraction grating with a period of 1200 lines/mm was employed to achieve high-resolution spectral data. A standard Renishaw CCD camera detector was utilized to record the Raman spectra, ensuring precise detection of the Raman shifts and providing reliable results for further analysis. Raman spectra were recorded over the range of 100÷3000 cm^{-1} (Figure 3).

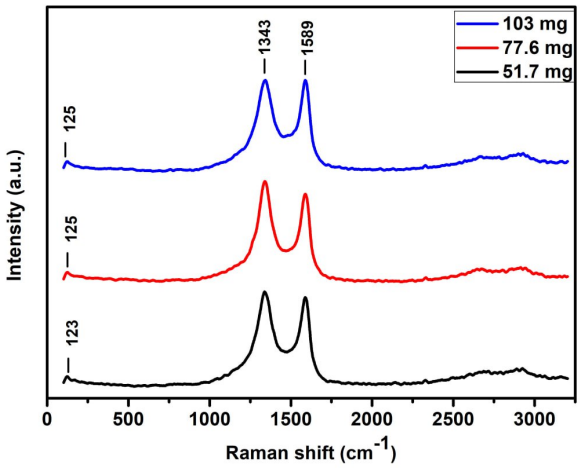

Figure 3. Raman spectrum of carbon nanotubes

From Figure 3, it is established that, with the same process of carbon nanotube growth, the mass of the catalyst does not affect the formation of carbon nanotubes. The peaks that characterize the most important properties of the Raman spectra of SWCNTs are: the RBM, observed in the range of 100÷300 cm^{-1}, the tangential G-band (characterizing the C-C bond) near the frequency of ~1572 cm^{-1} and the D-band caused by defects and disorder near the frequency of ~1300 cm^{-1} and its second-order harmonic (G'-band) in the frequency range of 2600÷2800 cm^{-1} [21]. As can be seen from Figure 3, the peaks characterizing SWCNTs are observed in the frequency ranges indicated above. Of these four properties, RBM is the property that is inversely proportional to the nanotube diameter, according to expression [22].

$$\omega_{RBM} = A/(dt) + B \quad (1)$$

Where: ω_{RBM} is the oscillation frequency, A and B are constants, and dt is the diameter of the carbon nanotube.

In addition, the quality of CNTs is evaluated by the ratio of the intensity of peak D to the intensity of peak G (I_D/I_G) [23]. If $I_D/I_G \approx 1$, it indicates the presence of more defects and low quality, and if $I_D/I_G < 1$, it indicates good quality of the synthesized CNTs. The influence of the catalyst layer, i.e. the mass of the catalyst, on the yield of the CNTs during the synthesis was also studied. The yield of the CNTs is calculated using formula (2) [24].

$$C_{yield} = (m_{tot} - m_{cat})/m_{cat} \cdot 100\% \quad (2)$$

Where: m_{tot} is the total mass, m_{cat} is the mass of the catalyst, C_{yield} is the yield of the CNTs.

In addition, the effect of catalyst layers on the masses of grown CNTs was studied (table 1).

Table 1. Effect of catalyst content on the yield of grown CNTs

Weight of NiO, (mg)	Weight of Ni, (mg)	Substrate	ω_{RBM} (cm^{-1})	I_D/I_G	d_t (nm)	Weight of CNTs, (g)	CNTs yield (%)
66	51.7	SiO_2 /Si	123	1.04	2.11	0.23	445
99	77.6		125	1.13	2.07	0.16	216
132	103		125	1.01	2.07	0.13	126

The analysis of the data in the table allows us to draw the following conclusions. When using the Ni catalyst mass of 51.7 mg, the RBM peak frequency was 123 cm^{-1}, the peak D intensity ratio was 1,04, and carbon nanotubes with a diameter of 2.11 nm and a mass of 0.23 were synthesized. With an increase in the catalyst mass to 77.6 mg, the RBM

peak frequency was 125 cm^{-1}, the peak D intensity ratio was 1.13, the diameter was reduced to 2,07 nm and the mass of the synthesized carbon nanotube was 0,16 grams. With a further increase in the catalyst mass to 103 mg, the RBM peak frequency was 125 cm^{-1}, the peak D intensity ratio was 1.01, the diameter of the carbon nanotubes was reduced to 2.07 nm, and the mass of the synthesized carbon nanotube was 0.13 grams.

The study shows that the catalyst layers affect the properties of the synthesized carbon nanotubes. A large number of catalyst layers increases the RBM peak frequency and decreases the diameter of carbon nanotubes. At the same time, a decrease in the catalyst layers leads to an increase in the mass of the synthesized carbon nanotubes. This conclusion is confirmed by the fact that the yield of CNTs according to formula (2) was also 445%, 216% and 126%, respectively.

CONCLUSIONS

In this study, the influence of the nanocatalyst/substrate interface on the yield and phase quality of CNTs synthesized by the CVD method was determined. During the reduction of NiO nanoparticles – prepared via the sol–gel spin-coating technique and deposited on the substrate surface in different masses - active nickel catalytic centers were formed, which subsequently governed the growth efficiency of the CNTs.

Analyses revealed that increasing the catalyst mass reduces the diameter of single-walled CNTs and increases the RBM frequency, while the overall yield decreases. The highest yield, 445%, was obtained using 51,7 mg of catalyst. XRD and Raman spectroscopy results confirmed that the synthesized nanotubes possessed a crystalline structure and exhibited characteristic vibrational bands. Furthermore, it was demonstrated that, within the substrate/oxide layer/catalyst triple interface, stress relaxation occurred and nickel silicidation was effectively suppressed.

Overall, the findings indicate that the catalyst coating thickness, the thickness of the native oxide layer, and its uniform distribution across the substrate surface play a decisive role in controlling CNTs growth efficiency, diameter, and phase quality.

Acknowledgments

The authors gratefully acknowledge the financial and technical support provided by the Ministry of Higher Education, Science, and Innovation under project number IL-5421101842.

ORCID

Ilyos J. Abdisaidov, https://orcid.org/0000-0001-7473-1074; **Ilyos Kh. Khudaykulov,** https://orcid.org/0000-0002-2335-4456
Khatam B. Ashurov, https://orcid.org/0000-0002-7604-2333

REFERENCES

[1] M. Diarra, *et al*., Physical Review Letters, **109**(18), 185501 (2012). https://doi.org/10.1103/PhysRevLett.109.185501
[2] B. Karakashov, M. Mayne-L'Hermite, and M. Pinault, Nanomaterials, **12**(13), 2300 (2022). https://doi.org/10.3390/nano12132300
[3] X. Zhao, *et al*., Accounts of chemical research, **55**(23), 3334 (2022). https://doi.org/10.1021/acs.accounts.2c00592
[4] D. Hedman, *et al*., Nature Communications, **15**(1), 4076 (2024). https://doi.org/10.1038/s41467-024-47999-7
[5] K. Awasthi, A. Srivastava, and O. N. Srivastava, Journal of nanoscience and nanotechnology, **5**(10), 1616-1636 (2005). https://doi.org/10.1166/jnn.2005.407
[6] E.R. Meshot, *et al*., Acs Nano, **3**(9), 2477 (2009). https://doi.org/10.1021/nn900446a
[7] L. Nánai, *et al*., Scientific Reports, **14**(1), 7307 (2024). https://doi.org/10.1038/s41598-024-57862-w
[8] J. Bora, *et al*., Applied Surface Science, **648**, 158988 (2024). https://doi.org/10.1016/j.apsusc.2023.158988
[9] J. Sengupta, and C. M. Hussain, Biosensors, **15**(5), 296 (2025). https://doi.org/10.3390/bios15050296
[10] S. Zecchi, *et al*., Micromachines, **16**(1), 53 (2024). https://doi.org/10.3390/mi16010053
[11] K.J. Hughes, *et al*., ACS Applied Nano Materials, **7**(16), 18695 (2024). https://doi.org/10.1021/acsanm.4c02721
[12] A. Venkataraman, *et al*., Nanoscale research letters, **14**(1), 220 (2019). https://doi.org/10.1186/s11671-019-3046-3
[13] Y. Hoshino, *et al*., Nuclear Instruments and Methods in Physics Research Section B: Beam Interactions with Materials and Atoms, 282, 125 (2012). https://doi.org/10.1016/j.nimb.2011.08.062
[14] X. Li, *et al*., Scientific Reports, **8**(1), 4349 (2018). https://doi.org/10.1038/s41598-018-22467-7
[15] Y. Lin, *et al*., Nature Electronics, **6**(7), 506 (2023). https://doi.org/10.1038/s41928-023-00983-3
[16] M. Parashar, V.K. Shukla, and R. Singh, Journal of Materials Science: Materials in Electronics, **31**(5), 3729 (2020). https://doi.org/10.1007/s10854-020-02994-8
[17] A.A. Ismatov, C. Romanitan, Kh.B. Ashurov, M.M. Adilov, and A.A. Rahimov, Eurasian Physical Technical Journal, **22**(3(53)), 5 (2025). https://doi.org/10.31489/2025N3/5-13
[18] A.A. Rakhimov, I.K. Khudaykulov, A.A. Ismatov, and M.M. Adilov, East European Journal of Physics, (3), 436-441 (2025). https://doi.org/10.26565/2312-4334-2025-3-47
[19] W.H. Tan, S.L. Lee, and C.T. Chong, Key Engineering Materials, **723**, 470 (2017). https://doi.org/10.4028/www.scientific.net/KEM.723.470
[20] S.P. Chai, S.H.S. Zein, and A.R. Mohamed, Diamond and related materials, **16**(8), 1656 (2007). https://doi.org/10.1016/j.diamond.2007.02.011
[21] Y. Guo, G. Zhai, Y. Ru, C. Wu, X. Jia, Y. Sun, *et al*., AIP Advances, **8**(3), 035111 (2018). https://doi.org/10.1063/1.5020936
[22] L.A. Bokobza, and J. Zhang, Express Polymer Letters, **6**(7), 601 (2012). https://doi.org/10.3144/expresspolymlett.2012.63
[23] A. C. Sparavigna, *et al*., International Journal of Sciences, 13(7), 1-26 (2024). https://doi.org/10.26434/chemrxiv-2024-xw377
[24] F. Taleshi *et al*., Fullerenes, Nanotubes and Carbon Nanostructures, **22**(10), 921 (2014). https://doi.org/10.1080/1536383X.2012.749456

ПІДВИЩЕННЯ ВИХОДУ ВУГЛЕЦЕВИХ НАНОТРУБОК ЧЕРЕЗ ІНТЕРФЕЙС НАНОКАТАЛІЗАТОР-СУБСТРАТ

Ільос Дж. Абдісаїдов, Севара Г. Гуломджанова, Ільос Х. Худайкулов, Хатам Б. Ашуров

Інститут іонно-плазмових та лазерних технологій імені У.А. Аріфова, Академія наук Республіки Узбекистан, 100125, вул. Дурмон йулі, 33, Ташкент, Узбекистан

У цьому дослідженні досліджувався вплив межі розділу нанокаталізатор/субстрат на вихід та якість вуглецевих нанотрубок (CNTs), синтезованих методом хімічного осадження з парової фази (CVD). Наночастинки оксиду нікелю (NiO) були отримані методом золь-гель спін-покриття та нанесені у вигляді тонких плівок з різною масою (66 мг, 99 мг та 132 мг) на підкладки SiO_2/Si з однаковою площею поверхні 12,56 см^2. Тонкі плівки наночастинок NiO на поверхні підкладки потім поміщали в CVD-реактор та відновлювали в атмосфері водню, що призводило до утворення наночастинок нікелю, які діяли як активні каталізатори під час синтезу вуглецевих нанотрубок. Пари етанолу використовувалися як єдине джерело вуглецю без будь-якого газу-носія, що дозволило точно та порівняльно оцінити вихід вуглецевих нанотрубок. Для характеристики отриманих вуглецевих нанотрубок використовували рентгенівську дифракцію (XRD) та раманівську спектроскопію. Результати XRD показали, що вуглецеві нанотрубки з високою кристалічністю утворювалися при використанні тонкої плівки каталізатора масою 51,7 мг. Раманівська спектроскопія підтвердила наявність піків RBM, G, D та G′, характерних для структур вуглецевих нанотрубок. Збільшення маси каталізатора призвело до зростання частоти RBM та зменшення діаметра вуглецевих нанотрубок. Однак збільшення маси каталізатора також призвело до зниження виходу вуглецевих нанотрубок. Найвищий вихід (445%) спостерігався для нанокаталізаторів Ni масою 51,7 мг. Ці результати демонструють, що товщина шару каталізатора та його поверхнева щільність розподілу на підкладці відіграють вирішальну роль у визначенні ефективності росту та структурної якості вуглецевих нанотрубок.

Ключові слова: *вуглецеві нанотрубки; NiO-каталізатор; золь-гель метод; CVD; межа між підкладкою та нанокаталізатором; RBM; вихід*